Acta Crystallographica Section D
Biological Crystallography
ISSN 0907-4449

Preliminary crystallographic characterization of BSAP, an extracellular aminopeptidase from *Bacillus subtilis*

Vera Reiland,[a] Yifat Fundoiano-Hershcovitz,[b] Gali Golan,[a] Rotem Gilboa,[a] Yuval Shoham[b] and Gil Shoham[a]*

[a]Department of Inorganic Chemistry and the Laboratory for Structural Chemistry and Biology, The Hebrew University of Jerusalem, Jerusalem 91904, Israel, and [b]Department of Biotechnology and Food Engineering and Institute of Catalysis Science and Technology, Technion-Israel Institute of Technology, Haifa 32000, Israel

Correspondence e-mail: gil2@vms.huji.ac.il

Received 27 August 2004
Accepted 24 October 2004

The extracellular aminopeptidase from *Bacillus subtilis* (BSAP) has recently been cloned, overexpressed and purified from *Escherichia coli*. It is a monomer with a molecular weight of 46 425 Da, consisting of 425 amino-acid residues and a double-zinc catalytic centre. The recombinant enzyme was found to be stable for 20 min at 353 K, to function optimally in the pH range 8–9 and to prefer basic and large hydrophobic N-terminal amino acids in peptide and protein substrates. As such, this enzyme can be used as a representative model for structural, functional and mechanistic studies of monomeric double-zinc aminopeptidases, many of which have been found to be involved in medically important biological activities. In this report, the crystallization and preliminary crystallographic characterization of wild-type BSAP are described. Two different crystal forms are reported, of which the hexagonal form H2 is the more suitable for structural study, with average unit-cell dimensions $a = b = 226.5$, $c = 42.8$ Å. A full diffraction data set has been collected from such a crystal of the native enzyme (2.2 Å resolution, 91.2% completeness, $R_{\rm merge} = 7.1\%$). A multiwavelength anomalous diffraction (MAD) data set was collected on native (zinc-containing) BSAP at three wavelengths around the zinc absorption edge (peak data set at 2.5 Å resolution, 98.8% completeness, $R_{\rm merge} = 5.3\%$). These diffraction data were collected at 95–100 K using a synchrotron X-ray source and a CCD area detector. The data are currently being used to obtain crystallographic phasing and to determine the detailed three-dimensional structure of the enzyme.

1. Introduction

Peptidases and proteinases are usually categorized according to the central catalytic component in their active site. The best known are those of serine proteinases, cysteine proteinases, aspartic proteinases and, to a lesser extent, metalloproteinases (Barrett, 2001). Peptidases can also be categorized on the basis of the relative position of their peptide cleavage: exopeptidases for a terminal amino-acid cleavage (aminopeptidases or carboxypeptidases) and endopeptidases for a cleavage of peptide bonds in other parts of the polypeptide chain. Of these categories and families of proteolytic enzymes, the least characterized group are the metallo-aminopeptidases. For example, while representatives of most classes of endopeptidases and carboxypeptidases were structurally analyzed during the 1960s–1980s, the first aminopeptidase structure was only determined in 1990 (Burley *et al.*, 1990). Nonetheless, aminopeptidases have been shown to be widely distributed in all organisms from bacteria to mammals, where they are present intracellularly, on the surface of cell membranes or excreted extracellularly (Taylor, 1996; Barrett, 2001; Wilk *et al.*, 2002). Aminopeptidases vary in size and specificity and have been shown to function in the metabolism and processing of many biologically important peptides and proteins. These enzymes are involved in a wide range of biological reactions such as protein digestion, protein maturation, protein degradation, hormone-level regulation and cell-cycle control. Aminopeptidases are therefore key players in many abnormal conditions and diseases including inflammation, cancer, cataracts, cystic fibrosis, strokes, diabetes and bacterial infections (Taylor, 1993*a*,*b*, 1996; Holz *et al.*, 2003). The full understanding of the biochemical activity, the detailed three-dimensional structure and the catalytic mechanism of action of aminopeptidases, and especially the factors that are critical for their proper biological function, are hence very important for a wide range of medical and pharmacological purposes.

Only partial information is currently available concerning the structure–function relationships and the catalytic mechanism of aminopeptidases, probably owing to the relatively limited structural information that is

available for these enzymes. The full three-dimensional structure of only four such enzymes has been reported so far, the bovine lens leucine aminopeptidase (LAP; Burley *et al*., 1990, 1992; Strater & Lipscomb, 1995) and the bacterial enzymes *Escherichia coli* methionine aminopeptidase (MAP; Roderick & Matthews, 1993; Lowther *et al.*, 1999), *Aeromonas proteolytica* aminopeptidase (AAP; Chevrier *et al.*, 1994, 1996) and *Streptomyces griseus* aminopeptidase (SGAP; Greenblatt *et al.*, 1997; Gilboa *et al.*, 2000). Structural information has recently been made available also for *E. coli* proline aminopeptidase (PAP; Wilce *et al.*, 1998). A common functional element that appears to be central to all of these enzymes is an active centre built of two metal ions (usually zinc). These metal ions are held in position by the side chains of amino-acid residues (usually glutamic acid, aspartic acid and histidine) of the protein around the active site, some of which bridge between the two metal ions.

One of the double-metal aminopeptidases that has contributed valuable information towards the understanding of their molecular mode of action is SGAP, a relatively small aminopeptidase isolated from the extracellular extracts of *S. griseus* (Spungin & Blumberg, 1989; Maras *et al*., 1996). It is a monomeric double-zinc enzyme for which the three-dimensional structure has been determined for both the native enzyme (Almog *et al.*, 1993; Greenblatt *et al.*, 1997; Papir *et al.*, 1998) and its complexes with various analogues (Gilboa *et al.*, 2000, 2001; Reiland *et al.*, 2004). These structures demonstrated that the active site of the enzyme contains two adjacent pentacoordinated zinc cations which are about 3.6 Å apart. In the uncomplexed form of this enzyme, the two zinc ions are bridged by a water molecule, which was found to be removed upon binding of substrates or analogues (Gilboa *et al.*, 2000, 2001; Reiland *et al.*, 2004). A general catalytic mechanism has been proposed on the basis of these structures (Gilboa *et al.*, 2001) and the specific assignment of some of the catalytic residues has subsequently been confirmed by site-directed mutagenesis experiments (Fundoiano-Hershcovitz *et al.*, 2004*a*). Nevertheless, the detailed mechanism of catalysis of SGAP is not fully understood as yet, nor it is clear how relevant the proposed catalytic elements are to the general mode of action of double-zinc aminopeptidases.

A search of sequence databases was performed in order to find double-zinc aminopeptidases that are homologous to SGAP. A series of such enzymes is expected to clarify, at least in part, the degree to which the active site and the proposed mechanistic scheme of SGAP are general to other aminopeptidases of varying homology and substrate specificity. The search indicated that BSAP, a putative protein encoded by the *ywad* gene of *Bacillus subtilis*, shows relatively high sequence homology (over 30% identity) to SGAP, despite the significant difference in the overall size of the two proteins (Maras *et al.*, 1996; Greenblatt *et al.*, 1997). The *ywad* gene product, BSAP, has recently been cloned, overexpressed and purified from *E. coli* and confirmed to be a double-zinc aminopeptidase (Fundoiano-Hershcovitz *et al.*, 2004*b*). The recombinant enzyme (monomer, MW 46 425 Da, 425 amino acids) was found to be stable for 20 min at 353 K, to function optimally in the pH range 8–9 and to prefer a basic and large hydrophobic amino acid as the N-terminal residue in synthetic model substrates.

In this report, we describe the crystallization of BSAP and the preliminary crystallographic characterization of the resulting BSAP crystals. Two major crystal forms have been obtained from the recombinant wild-type enzyme, one of which (the H2 form) was found to be of sufficient quality and stability for high-resolution structural analysis. A complete MAD data set (at the zinc absorption edge) has been collected from these crystals to 2.5 Å resolution together with a non-MAD data set which was measured at 2.2 Å resolution. These data sets will be used for phase determination and three-dimensional structure determination of the native BSAP protein.

2. Experimental

2.1. Purification of BSAP

Wild-type BSAP was purified from an overexpressing strain of *E. coli* as described in detail elsewhere (Fundoiano-Hershcovitz *et al.*, 2004*b*). Briefly, the *E. coli* BL21(DE3) cells , containing the *ywad* gene cloned into the pET9d vector, were grown in Terrific Broth medium supplemented with kanamycin (25 µg ml^{-1}). At a culture density of OD_{600} = 0.6, isopropyl β-D-thiogalactopyranoside (IPTG) was added (1 m*M*) and growth was maintained for 12–16 h. Cells from 1 l overnight culture were harvested, resuspended in 15 ml 100 m*M* NaCl, 50 m*M* MOPS buffer pH 7.5, 0.02% sodium azide, and disrupted by three passages through a French press at room temperature. The soluble fraction (about 30 ml) containing the recombinant BSAP was diluted with water by a factor of 10 in order to decrease the ionic strength and viscosity. The diluted fraction was then applied onto a HiPrep SP Sepharose Fast Flow XK 16/10 column on an ÄKTA Explorer (Pharmacia). The column was washed with four column volumes (20 × 4 ml) of a solution containing 100 m*M* NaCl, 50 m*M* MOPS, 0.02% sodium azide pH 7.5 and the protein was eluted with a linear NaCl gradient (100 m*M*–1.5 *M*) over 20 column volumes. Kinetic measurements of the purified recombinant BSAP were carried out by continuous and/or stopped assay procedures using L-leucine-*para*-nitroanilide (Leu-pNA; Sigma) as a substrate. The catalytic reaction was followed *via* the increase in absorbance of one of the products, *para*-nitroanilide (pNA), at 405 nm, using an extinction coefficient of $\Delta\varepsilon$ = 9.65 mM^{-1} cm^{-1} for pNA at pH 8 (Fundoiano-Hershcovitz *et al.*, 2004*b*). These measurements were performed in order to confirm the full enzymatic activity of the protein sample just before its crystallization.

2.2. Crystallization experiments

Crystallization experiments were set up immediately after the last purification step of the recombinant BSAP protein. The purified protein was concentrated using Centricon centrifugal concentrators (Millipore, MA, USA) to approximately 15 mg ml^{-1}. All initial crystallization experiments were performed by the hanging-drop vapour-diffusion method, using an extensive series of different factorial screens (Jancarik & Kim, 1991). In general, these initial conditions were based on commercially available sets of screens. Once positive results were obtained, further refinement of these crystallization conditions were performed with specially prepared solutions, optimizing parameters such as pH, ionic strength and protein concentration (Almog *et al.*, 1993, 1994; Teplitsky *et al*., 1997, 1999, 2000).

The final BSAP protein crystallization drops were prepared by mixing the concentrated protein solution with an equal amount of each of the specific screen conditions to give a final drop volume of 6 µl. Each of these protein drops was suspended over a 1 ml reservoir solution in 4 × 6 VDX crystallization plates (Hampton Research, CA, USA) for a period of about 14–60 d. A number of different crystal forms were obtained from these initial experiments, but only two of them (H1 and H2) were found to be suitable for further crystallographic analysis (see below).

Processing, reduction, indexing, integration and scaling of the diffraction data were conducted using the *DENZO* and *SCALE-*

PACK crystallographic programs (Otwinowski, 1993; Otwinowski & Minor, 1997).

3. Results and discussion

3.1. Characterization of the H1 crystal form

The first crystal form of native BSAP was initially obtained by the hanging-drop methods described above, using a reservoir solution consisting of high concentrations of ammonium sulfate (2.2–2.5 *M*; no buffer or other additives). This form was later identified as a member of the hexagonal crystal system and was hence identified as H1. Efforts to refine the crystallization conditions of this form resulted in three different crystal habits, with three different crystal morphologies (see examples for crystal forms and habits in Almog *et al.*, 1991; Gilboa *et al.*, 1998; Bar *et al.*, 2004; Golan *et al.*, 2004). Since they all generally looked like lenses, these three crystal habits were termed L1, L2 and L3, all of which confirmed to have the general crystallographic characteristics of the H1 crystal form (Table 1). As shown below, none of these crystal habits turned out to be suitable for a full crystal structure analysis at a reasonable resolution.

The first such type of crystal (H1 form, L1 habit) was obtained at room temperature with the original reservoir solution of 2.4 *M* ammonium sulfate and a 1:1 mixture of protein and reservoir in the drops. These crystals could be observed after about one week and grew to full size after another few days. These L1 crystals (Fig. 1*a*) usually appear as colourless flat lenses with curved convex faces and sharp points at the two poles. In most of the experiments about two to six crystals grew in one drop, all of which were of similar size and shape. Typical dimensions of these crystals are 0.4 × 0.2 × 0.1 mm, where the long dimension reflects the pole-to-pole distance. Several such crystals were tested for X-ray diffraction data collection but did not give diffraction of sufficient quality for a full crystallographic characterization.

Table 1
Representative crystallization characteristics of crystal forms H1 and H2 of BSAP.

Crystal habit	H1 (L2)	H2
Protein concentration (mg ml^{-1})	15	18
Crystallization solution	2.4 *M* ammonium sulfate, 5% glycerol	4 m*M* manganese chloride, 0.1 *M* sodium acetate buffer, 0.2 *M* lithium sulfate, 25%(*w*/*v*) PEG 2K MME
pH	6.5	5.5
No. of crystals in the drop	2–6	10–15
Growth period (d)	5–7	12–16
Crystal dimensions (mm)	0.5 × 0.15 × 0.08	0.3 × 0.05 × 0.05

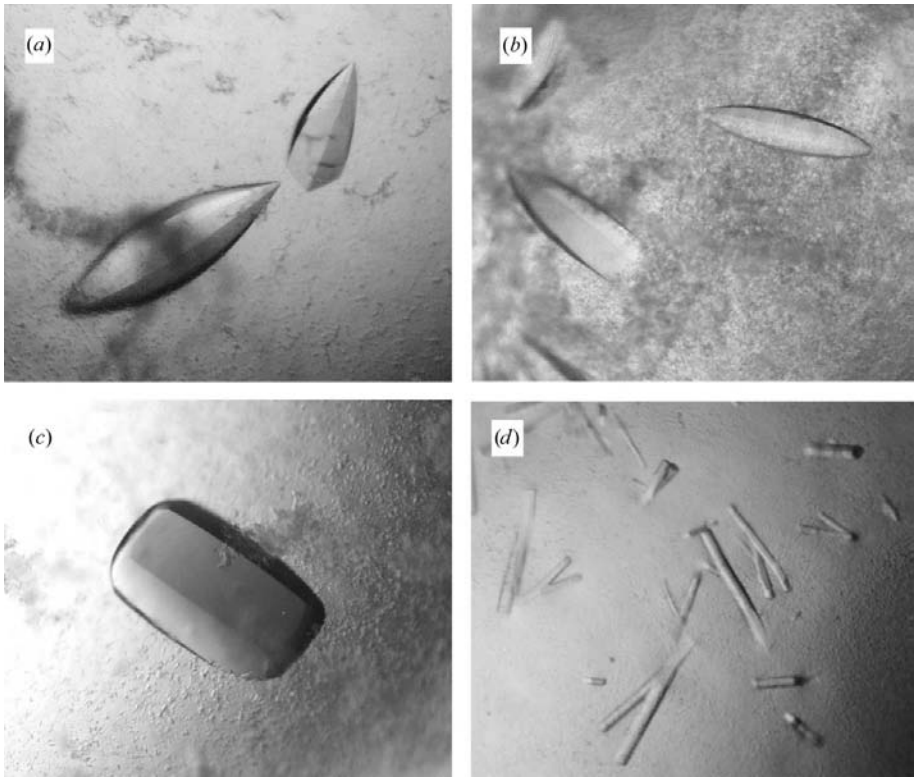

Figure 1
The four crystal habits obtained for wild-type BSAP. (*a*) The L1 habit of the H1 crystal form (typical crystal dimensions 0.4 × 0.2 × 0.1 mm). (*b*) The L2 habit of the H1 crystal form (typical crystal dimensions 0.5 × 0.15 × 0.08 mm). (*c*) The L3 habit of the H1 crystal form (typical crystal dimensions 0.4 × 0.3 × 0.15 mm). (*d*) Crystals of the H2 crystal form (typical crystal dimensions 0.3 × 0.05 × 0.05 mm). These crystals were used for the measurement of a full diffraction data set at 2.2 Å resolution. Magnifications used for these pictures are about ×50 to ×90.

Refinement of the crystallization conditions of the H1/L1 crystals with various additives led to a second type of crystals of the H1 crystal form (L2 habit; Fig. 1*b*). These L2 crystals were obtained by the hanging-drop methods described above (at room temperature) using a reservoir consisting of 2.4 *M* ammonium sulfate and low concentrations (2–6%) of glycerol. The best crystals of this habit were obtained with an initial solution of 5% glycerol (Table 1) and could be observed after about a week. These crystals have also the general shape of lenses, but are considerably more elongated (along the pole-to-pole axis) than those of the L1 habit, with typical dimensions of 0.5 × 0.15 × 0.08 mm. These crystals were found to be rather sensitive to radiation damage, but their diffraction appeared to be reasonable, at least for a full data-set measurement (see below).

Over a course of 4–9 months the H1/L2 crystals gradually transform into another type of crystals (L3 habit), which are thicker and more transparent than the original L2 crystals. They usually look like small rectangular 'boxes' with some curved surfaces, but mostly flat and defined faces, with typical dimensions of 0.4 × 0.3 × 0.15 mm (Fig. 1*c*). Several such crystals were tested for X-ray diffraction, which appeared to be very diffuse and limited to resolutions of less than 4.5 Å. Such diffraction characteristics were not sufficient for detailed crystallographic characterization.

The observations presented above indicated that of the crystal habits of the H1 crystal form, only the L2 crystals are of practical potential for crystal structure analysis. Several L2 crystals were therefore used for more detailed crystallographic characterization and measurement of X-ray diffraction data under cryogenic conditions. These experiments were performed using

X-ray synchrotron radiation (λ = 1.10 Å) and a CCD area detector (Quantum-4, ADSC Inc., USA) at the X25 beamline of the National Synchrotron Light Source facility (NSLS), Brookhaven National Laboratory (NY, USA).

The crystal-freezing procedure used for these experiments included a short soaking of the target crystal (about 2–3 min) in a cryoprotectant solution containing the original crystallization reservoir solution (2.4 *M* ammonium sulfate, 5% glycerol) and 20%(*v*/*v*) glycerol. The presoaked crystal was then submitted to immediate flash-freezing, directly within a cold nitrogen-gas stream (95 K, Oxford Cryosystem). The observed diffraction pattern of some of these crystals exceeded the 3.8 Å resolution limit. The observed diffraction pattern indicated that the crystals belong to a primitive hexagonal crystal system (space group $P6_122$), with average crystallographic unit-cell dimensions $a = b = 117.86$, $c = 254.14$ Å. Different crystals from this batch gave similar unit-cell dimensions, with an overall deviation of less than 0.3% from these average values. A number of alternative freezing procedures have been tested in order to improve the resolution and quality of the diffraction of these crystals, including their short soaking in various heavy oils. Unfortunately, these efforts have so far been unsuccessful.

One such crystal was used for a full X-ray diffraction data measurement. An oscillation data set ($\Delta\varphi = 0.5^\circ$) was measured on a single crystal at the NSLS/X25 beamline (λ = 1.10 Å, 95 K). The raw CCD diffraction images were processed with the *DENZO* and *SCALEPACK* software packages (Otwinowski, 1993). A total of 38 896 accepted reflections [$F > 0\sigma(F)$] were measured in the 40.0–3.80 Å resolution range and resulted in 10 616 independent reflections with 97.2% completeness to 3.80 Å resolution (98.8% completeness for the highest resolution shell of 3.87–3.80 Å). The overall redundancy in the combined data set was 4, the overall mosaicity was 0.43, the average $\langle I/\sigma(I)\rangle$ was 5.9 and the final $R_{\rm merge}$ for the whole data was 9.5% (Table 2).

The volume of the H1/L2 crystallographic unit cell, as determined from the mean value of the unit-cell dimensions at 95 K is 3.06×10^6 Å^3. Assuming that the specific ratio of volume to protein in the crystal ($V_{\rm M}$) is within the normal range of $V_{\rm M}$ values observed for soluble protein crystals (1.68–3.5 Å^3 Da^{-1}; Matthews, 1968), there should be two or three BSAP monomers (425 amino acids; MW 46 425 Da) in the crystallographic asymmetric unit (space group $P6_122$; 24 or 36 monomers per unit cell). With two molecules in the H1 asymmetric unit (24 in the unit cell), the calculated $V_{\rm M}$ is 2.76 Å^3 Da^{-1} and the corresponding solvent content in the crystals is 54.8%. With three molecules in the asymmetric unit (36 in the unit cell), the calculated $V_{\rm M}$ is 1.83 Å^3 Da^{-1} and the corresponding solvent content in the crystals is 32.3%. Of these two possibilities, the former seems the more probable.

Table 2
Selected crystallographic parameters for the H1 and H2 crystal forms of BSAP.

Values in parentheses are for the last resolution shell.

		H2		
Crystal form	H1	Inflection	Peak	Remote
Wavelength	1.100	1.2828	1.2822	0.9393
Crystal system	Primitive hexagonal	Primitive hexagonal	Primitive hexagonal	Primitive hexagonal
Unit-cell dimensions (Å)				
a	117.86	226.16	226.01	226.53
c	254.14	42.69	42.67	42.76
Space group	$P6_122$	$P6_3$	$P6_3$	$P6_3$
Oscillation angle per frame (°)	0.5	0.25	0.25	0.25
Exposure time per frame (s)	90	5	5	2
No. of frames	128	240	240	240
Data-collection temperature (K)	95	100	100	100
Resolution range (Å)	40–3.80 (3.87–3.80)	60–2.50 (2.54–2.50)	60–2.50 (2.54–2.50)	60–2.20 (2.24–2.20)
No. of reflections	38896	147411	148919	179017
No. of unique reflections	10616	42775	42382	58386
$\langle I/\sigma(I)\rangle$	5.9	11.8	13.1	14.4
Completeness (%)	97.2 (98.8)	97.5 (71.1)	98.8 (86.3)	91.2 (45.6)
$R_{\rm merge}$ (%)	9.5 (43.1)	5.5 (25.7)	5.3 (20.5)	7.1 (38.5)

3.2. Characterization of the H2 crystal form

As shown above, the potential of the H1 crystal form of BSAP for meaningful study of its structure and catalytic mechanism seems to be rather limited, mainly because of the low resolution (3.8 Å for the H1/L2 form) and poor quality of the diffraction and the difficulties in the crystal-freezing procedures. It was therefore clear that an alternative crystal type should be obtained and/or an alternative crystal-freezing procedure should be developed. Unfortunately, further refinement of the original crystallization conditions and the freezing procedures of the H1 form did not result in significant improvement in either the diffraction quality or the crystal-freezing effectiveness. For example, systematic variations around the reported procedures indicated that the crystals are extremely sensitive to additions of cryosolvents such as glycerol and polyethylene glycol (PEG).

In order to find new and different starting conditions for BSAP crystallization, a new round of screening for crystallization conditions of native BSAP was conducted, utilizing new series of solutions of different buffers, precipitants, salts and other additives. These screens led to a new crystal form (H2), which was obtained at pH 5.5 using polyethylene glycol (PEG 2K MME, 20–30%) as a precipitant and 0.2 *M* lithium sulfate as a salt additive. Further refinement of these initial conditions demonstrated that the best H2 crystals were obtained by the hanging-drop method using a reservoir solution made of 25% PEG 2K MME, 0.2 *M* lithium sulfate, 4 m*M* manganese chloride and 0.1 *M* sodium acetate buffer at pH 5.5. Under these conditions at room temperature, the H2 crystals could first be observed after about two weeks, growing to their full size (about 10–15 crystals per drop) after another week. These H2 crystals (Fig. 1*d*) usually appear as colourless transparent elongated needles with a square cross-section, defined faces and sharp edges. Typical dimensions of these crystals are $0.3 \times 0.05 \times 0.05$ mm, but the long dimension along the needle axis can vary over the range 0.2–0.5 mm.

Several H2 crystals were used for initial crystallographic characterization and measurement of X-ray diffraction data under cryogenic conditions. These experiments were performed using X-ray synchrotron radiation and a CCD area detector (Quantum-4, ADSC) at the ID14-4 beamline of the European Synchrotron Radiation Facility (ESRF; Grenoble, France). All diffraction data were indexed, integrated, corrected and merged with the *DENZO* and *SCALEPACK* programs (Otwinowski & Minor, 1997), to give the final intensity data sets. Representative data-collection and data-processing parameters are listed in Table 2.

The H2 crystal form appeared to be much easier to freeze than the H1 form, mainly

since its initial mother liquor contained 25% PEG 2K MME, a solution composition that can undergo supercooling without further treatment. Hence, these crystals could be taken from the crystallization drop and immediately placed into a temporarily blocked cold nitrogen-gas stream (100 K, Oxford Cryosystem), allowing a quick and smooth flash-freezing of each crystal directly on the beamline goniometer head, just prior to data collection. Attempts were made to improve the freezing procedure with presoaking of the crystals in the original solution, followed by small additions of cryoprotectants such as glycerol and other types of PEG. Unfortunately, none of these modified procedures showed significant improvement in the quality or resolution of the diffraction pattern.

The direct crystal-freezing procedure enabled a full X-ray diffraction data measurement on one crystal of the H2 form, using the ESRF/ID14-4 high-intensity beamline (λ = 0.9393 Å, 100 K) and an automatic oscillation method ($\Delta\varphi = 0.5^\circ$). The raw CCD diffraction images were processed with the *DENZO* and *SCALEPACK* software packages (Otwinowski, 1993). A total of 179 017 accepted reflections [$F > 0\sigma(F)$] were measured in the 60.0–2.20 Å resolution range and resulted in 58 386 independent reflections with 91.2% completeness to 2.20 Å resolution. The overall redundancy of the combined data set was 4, the overall mosaicity was 0.43, the average $\langle I/\sigma(I)\rangle$ was 14.5 and the final $R_{\rm merge}$ for the whole data was 7.1%. The observed diffraction pattern indicated that the crystals belong to a primitive hexagonal crystal system (space group $P6_3$), with average unit-cell dimensions $a = b = 226.53$, $c = 42.76$ Å (Table 2).

The volume of the H2 crystallographic unit cell, as determined from the mean value of the unit-cell dimensions at 100 K, is 1.89×10^6 Å^3. Assuming that the specific ratio of volume to protein in the crystal is within the normal range of $V_{\rm M}$ values (Matthews, 1968), there should be two or three molecules of BSAP in the crystallographic asymmetric unit (space group $P6_3$; 12 or 18 monomers per unit cell). With two molecules in the H2 asymmetric unit, the calculated $V_{\rm M}$ is 3.40 Å^3 Da^{-1} and the corresponding solvent content in the crystals is 63.5%. Similarly, with three molecules in the asymmetric unit the calculated $V_{\rm M}$ is 2.26 Å^3 Da^{-1} and the corresponding solvent content is 45.2%. Both of these two possibilities seem to be quite probable according to Matthews (1968), although the case of three molecules seems more likely. The actual content of the unit cell will have to be determined at a later stage when clear electron-density maps are available.

As native BSAP has been shown to be a zinc aminopeptidase (Fundoiano-Hershcovitz *et al.*, 2004*b*) one can (in principle) use the anomalous signal of the two active-site zinc ions for a multiple anomalous diffraction (MAD) experiment at the zinc absorption edge (Hendrickson & Ogata, 1997). Although relatively weak, the zinc anomalous signal should be useful for crystallographic phase determination and/or improvement as well as for the corresponding crystal structure analysis (see, for example, Ennifar *et al.*, 2001). This is especially true for rather small proteins with two such zinc ions placed very close to each other (predicted Zn–Zn distance of about 3.5 Å).

Such a MAD experiment was performed on the same crystal that was used for the native data collection described above, using the data collected at λ = 0.9393 Å as the remote-wavelength data. The corresponding data sets at the peak (λ = 1.2822 Å) and inflection (λ = 1.2828 Å) points of the zinc edge were collected after the remote data set, using the same crystal orientation and data-collection setup. These two additional data sets were measured to a practical resolution of 2.50 Å (ESRF/ID14-4, 100 K) and showed only minimal radiation-damage effects. As for the original data, these diffraction data sets were indexed, integrated, corrected and merged with the *DENZO* and *SCALEPACK* programs (Otwinowski & Minor, 1997), to give two complete intensity data sets at both wavelengths. Representative data-collection and data-processing parameters are listed in Table 2. The MAD data sets are currently being used to obtain crystallographic phasing and to determine the detailed three-dimensional structure of BSAP, together with molecular-replacement calculations using the structure of native SGAP as a reference model.

We thank the staff at the National Synchrotron Light Source (NSLS, X25 beamline) of the Brookhaven National Laboratory and the staff at the European Synchrotron Research Facility (ESRF, ID14-4 beamline) for their helpful support during the X-ray synchrotron data measurement and analysis. This work was supported, in part, by a grant from the German Federal Ministry of Education, Science, Research and Technology (BMBF) and the Israeli Ministry of Science (MOS) under the aegis of GBF–Gesellschaft fur Biotechnologische Forschung GmbH, Braunschweig. It was also supported by the Otto Meyerhof Center for Biotechnology established by the Minerva Foundation (Munich, Germany), and by the Israel Academy of Sciences and Humanities–Israel Science Foundation (ISF). VR was supported by a Marie Curie Fellowship from the European Commission and by a Lady Davis Fellowship from the Hebrew University of Jerusalem, Israel.

References

Almog, O., Greenblatt, H. M., Spungin, A., Ben-Meir, D., Blumberg, S. & Shoham, G. (1993). *J. Mol. Biol.* **230**, 342–344.
Almog, O., Klein, D., Braun, S. & Shoham, G. (1994). *J. Mol. Biol.* **235**, 760–762.
Almog, O., Shoham, G., Michaeli, D. & Nechushtai, R. (1991). *Proc. Natl Acad. Sci. USA*, **88**, 5312–5316.
Bar, M., Golan, G., Teplitsky, A., Nechama, M., Zolotnitsky, G., Shoham, Y. & Shoham, G. (2004). *Acta Cryst.* D**60**, 545–549.
Barrett, A. J. (2001). *Proteolytic Enzymes*, edited by R. Beynon & J. S. Bond, pp. 12–21. Oxford University Press.
Burley, S. K., David, P. R., Sweet, R. M., Taylor, A. & Lipscomb, W. N. (1992). *J. Mol. Biol.* **224**, 113–140.
Burley, S. K., David, P. R., Taylor, A. & Lipscomb, W. N. (1990). *Proc. Natl Acad. Sci. USA*, **87**, 6878–6882.
Chevrier, B., D'Orchymont, H., Schalk, C., Tarnus, C. & Moras, D. (1996). *Eur. J. Biochem.* **237**, 393–398.
Chevrier, B., Schalk, C., D'Orchymont, H., Rondeau, J.-M., Moras, D. & Tarnus, C. (1994). *Structure*, **2**, 283–291.
Ennifar, E., Walter, P. & Dumas, P. (2001). *Acta Cryst.* D**57**, 330–332.
Fundoiano-Hershcovitz, Y., Rabinovitch, L., Langut, Y., Reiland, V., Shoham, G. & Shoham, Y. (2004*a*). *FEBS Lett.* **571**, 192–196.
Fundoiano-Hershcovitz, Y., Rabinovitch, L., Langut, Y., Reiland, V., Shoham, G. & Shoham, Y. (2004*b*). In preparation.
Gilboa, R., Bauer, A. & Shoham, G. (1998). *Acta Cryst.* D**54**, 1467–1470.
Gilboa, R., Greenblatt, H. M., Perach, M., Spungin-Bialik, A., Lessel, U., Wohlfahrt, G., Schomburg, D., Blumberg, S. & Shoham, G. (2000). *Acta Cryst.* D**56**, 551–558.
Gilboa, R., Spungin-Bialik, A., Wohlfahrt, G., Schomburg, D., Blumberg, S. & Shoham, G. (2001). *Proteins Struct. Funct. Genet.* **44**, 490–504.
Golan, G., Zharkov, D. O., Fernandes, A. S., Zaika, E., Kycia, J. H., Wawrzak, Z., Grollman, A. P. & Shoham, G. (2004). *Acta Cryst.* D**60**, 1476–1480.
Greenblatt, H. M., Almog, O., Maras, B., Spungin-Bialik, A., Barra, D., Blumberg, S. & Shoham, G. (1997). *J. Mol. Biol.* **265**, 620–636.
Hendrickson, W. A. & Ogata, C. M. (1997). *Methods Enzymol.* **276**, 494–523.
Holz, R. C., Bzymek, K. P. & Swierczek, S. I. (2003). *Curr. Opin. Chem. Biol.* **7**, 197–206.
Jancarik, J. & Kim, S.-H. (1991). *J. Appl. Cryst.* **24**, 409–411.

Lowther, W. T., Orville, A. M., Madden, D. T., Lim, S., Rich, D. H. & Matthews, B. W. (1999). *Biochemistry*, **38**, 7678–7688.
Maras, B., Greenblatt, H. M., Shoham, G., Spungin-Bialik, A., Blumberg, S. & Barra, D. (1996). *Eur. J. Biochem.* **236**, 843–846.
Matthews, B. W. (1968). *J. Mol. Biol.* **33**, 491–497.
Otwinowski, Z. (1993). *Proceedings of the CCP4 Study Weekend. Data Collection and Processing*, edited by L. Sawyer, N. Isaacs & S. Bailey, pp. 56–62. Warrington: Daresbury Laboratory.
Otwinowski, Z. & Minor, W. (1997). *Methods Enzymol.* **276**, 307–326.
Papir, G., Spungin-Bialik, A., Ben-Meir, D., Fudim, E., Gilboa, R., Greenblatt, H. M., Shoham, G., Lessel, U., Schomburg, D., Ashkenazi, R. & Blumberg, S. (1998). *Eur. J. Biochem.* **258**, 313–319.
Reiland, V., Gilboa, R., Spungin-Bialik, A., Schomburg, D., Shoham, Y., Blumberg, S. & Shoham, G. (2004). *Acta Cryst.* D**60**, 1738–1746.
Roderick, S. L. & Matthews, B. W. (1993). *Biochemistry*, **32**, 3907–3912.
Spungin, A. & Blumberg, S. (1989). *Eur. J. Biochem.* **183**, 471–477.
Strater, N. D. & Lipscomb, W. N. (1995). *Biochemistry*, **34**, 9200–9210.
Taylor, A. (1993*a*). *FASEB J.* **7**, 290–298.
Taylor, A. (1993*b*). *Trends Biochem. Sci.* **18**, 167–71.
Taylor, A. (1996). Editor. *Aminopeptidases*, pp. 1–20. Austin, Texas, USA: Landes Co.
Teplitsky, A., Feinberg, H., Gilboa, R., Lapidot, A., Mechaly, A., Shoham, Y., Stojanoff, V., Capel, M. & Shoham, G. (1997). *Acta Cryst.* D**53**, 608–611.
Teplitsky, A., Shulami, S., Moryles, S., Shoham, Y. & Shoham, G. (2000). *Acta Cryst.* D**56**, 181–184.
Teplitsky, A., Shulami, S., Moryles, S., Zaide, G., Shoham, Y. & Shoham, G. (1999). *Acta Cryst.* D**55**, 869–872.
Wilce, M. C., Bond, C. S., Dixon, N. E., Freeman, H. C., Guss, J. M., Lilley, P. E. & Wilce, J. A. (1998). *Proc. Natl Acad. Sci. USA*, **95**, 3472–3477.
Wilk, S., Wilk, E. & Magnusson, R. P. (2002). *Arch. Biochem. Biophys.* **407**, 176–183.